

# SCI: A Simple and Effective Framework for Symmetric Consistent Indexing in Large-Scale Dense Retrieval

Huimu Wang<sup>1</sup>, Yiming Qiu<sup>1,†</sup>, Xingzhi Yao<sup>1,†</sup>, Zhiguo Chen<sup>1</sup>,  
Guoyu Tang<sup>1</sup>, Songlin Wang<sup>1</sup>, Sulong Xu<sup>1</sup>, Mingming Li<sup>2</sup>

<sup>1</sup>JD.com, China, <sup>2</sup> Institute of Information Engineering, Chinese Academy of Sciences, China

liemingming@outlook.com

{wanghuimu1, qiuyiming3, yaoxingzhi1, chenzhiguo, tangguoyu, wangsonglin3, xusulong}@jd.com

## Abstract

Dense retrieval has become the industry standard in large-scale information retrieval systems due to its high efficiency and competitive accuracy. Its core relies on a coarse-to-fine hierarchical architecture that enables rapid candidate selection and precise semantic matching, achieving millisecond-level response over billion-scale corpora. This capability makes it essential not only in traditional search and recommendation scenarios but also in the emerging paradigm of generative recommendation driven by large language models, where semantic IDs-themselves a form of coarse-to-fine representation-play a foundational role. However, the widely adopted dual-tower encoding architecture introduces inherent challenges, primarily representational space misalignment and retrieval index inconsistency, which degrade matching accuracy, retrieval stability, and performance on long-tail queries. These issues are further magnified in semantic ID generation, ultimately limiting the performance ceiling of downstream generative models.

To address these challenges, this paper proposes a simple and effective framework named SCI comprising two synergistic modules: a symmetric representation alignment module that employs an innovative input-swapping mechanism to unify the dual-tower representation space without adding parameters, and an consistent indexing with dual-tower synergy module that redesigns retrieval paths using a dual-view indexing strategy to maintain consistency from training to inference. The framework is systematic, lightweight, and engineering-friendly, requiring minimal overhead while fully supporting billion-scale deployment. We provide theoretical guarantees for our approach, with its effectiveness validated by results across public datasets and real-world e-commerce datasets.

## CCS Concepts

• **Information systems** → **Novelty in information retrieval; Learning to rank; Recommender systems.**

† Corresponding author.

Permission to make digital or hard copies of all or part of this work for personal or classroom use is granted without fee provided that copies are not made or distributed for profit or commercial advantage and that copies bear this notice and the full citation on the first page. Copyrights for components of this work owned by others than the author(s) must be honored. Abstracting with credit is permitted. To copy otherwise, or republish, to post on servers or to redistribute to lists, requires prior specific permission and/or a fee. Request permissions from [permissions@acm.org](mailto:permissions@acm.org).  
Conference acronym 'XX, Woodstock, NY

© 2018 Copyright held by the owner/author(s). Publication rights licensed to ACM.  
ACM ISBN 978-1-4503-XXXX-X/2018/06  
<https://doi.org/XXXXXXX.XXXXXXX>

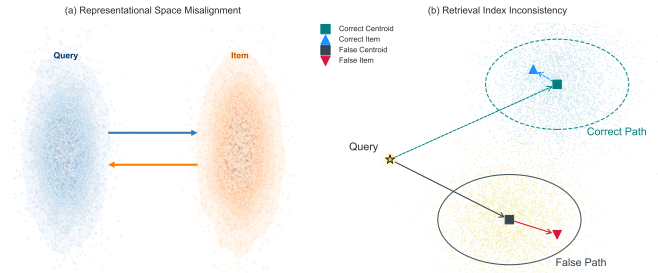


**Figure 1: The problem of space misalignment and index inconsistency in dual-tower retrieval.**

## Keywords

Retrieval Consistency, Embedding Alignment, Optimized Indexing

## ACM Reference Format:

Huimu Wang<sup>1</sup>, Yiming Qiu<sup>1,†</sup>, Xingzhi Yao<sup>1,†</sup>, Zhiguo Chen<sup>1</sup>, Guoyu Tang<sup>1</sup>, Songlin Wang<sup>1</sup>, Sulong Xu<sup>1</sup>, Mingming Li<sup>2</sup>, . 2018. SCI: A Simple and Effective Framework for Symmetric Consistent Indexing in Large-Scale Dense Retrieval. In *Proceedings of Make sure to enter the correct conference title from your rights confirmation email (Conference acronym 'XX)*. ACM, New York, NY, USA, 11 pages. <https://doi.org/XXXXXXX.XXXXXXX>

## 1 Introduction

In large-scale information retrieval/recommendation systems, dense retrieval has emerged as the industry standard due to its exceptional efficiency and competitive accuracy [8, 14, 15, 19, 29, 35]. At the heart of this approach lies a coarse-to-fine hierarchical retrieval architecture: by encoding queries and items into low-dimensional dense vectors, the system first rapidly narrows the search scope at a coarse level (e.g., via cluster centroids [14], graph navigation points [20], or primary quantization of semantic IDs [12]), and subsequently performs precise semantic matching at a fine-grained level (e.g., through residual quantization or nearest-neighbor distance comparison [30]). This hierarchical strategy enables millisecond-level responses over billion-scale corpora, forming the foundation for its practical deployment [3].

This capability not only makes dense retrieval highly effective in traditional recommendation and search scenarios but also establishes it as a cornerstone in the emerging paradigm of generative recommendation driven by large language models. It is particularly important to emphasize that semantic IDs—essential to generative models—are themselves a typical example of coarse-to-fine hierarchical representations. They are constructed using techniques such as hierarchical residual quantization (e.g., RQ-VAE [16, 23]).

However, the quality of the resulting discrete vocabulary is entirely dependent on the semantic space provided by the upstream dense retrieval system. The effectiveness of representation learning in dense retrieval directly determines the coherence of semantic IDs across coarse partitioning and fine-grained quantization, thereby defining the performance ceiling for subsequent generative models [16].

As the core architecture enabling dense retrieval, the dual-tower model learns separate vector representations for queries and items through independent encoder towers. This decoupled design is key to its efficiency and enables seamless integration with approximate nearest neighbor (ANN) search techniques [30]. However, this independent encoding mechanism also introduces inherent challenges, primarily manifested in two interrelated aspects:

1) **Representational Space Misalignment:** During training, the two towers operate with limited interactive supervision, causing their embeddings to occupy divergent vector subspaces and exhibit significant anisotropy (as shown in Fig 1). As a result, simple similarity measures often fail to capture true semantic relevance. Although contrastive learning and related techniques have been used to align positive pairs [14, 30], such alignment is often incomplete in practice or relies heavily on external data—as illustrated by the distribution shift between dual-tower embeddings. 2) **Retrieval Index Inconsistency:** The representational misalignment is further exacerbated during retrieval by the structure of the index. Popular indexing methods—including cluster-based IVF-PQ, graph-based HNSW, and semantic ID generation—all adopt a coarse-to-fine retrieval architecture. Due to space misalignment, the initial matching between a query and coarse-level structures (e.g., IVF centroids, HNSW entry points, or coarse semantic ID tokens) is biased from the start (query  $\rightarrow$  irrelevant cluster center  $\rightarrow$  items), confining subsequent fine-grained retrieval to incorrect neighborhoods and propagating errors throughout the process (as shown in Fig 1).

Critically, these inconsistencies become systematically embedded in the semantic ID generation process. Techniques like residual quantization [2] learn a hierarchical discrete representation of items based solely on item-item relationships, independent of query distributions. When the dual-tower representations are misaligned, the resulting semantic ID vocabulary is built upon biased item representations. Consequently, generative models inherit a fundamentally flawed semantic space, severely limiting the system's overall performance potential.

These inconsistencies impact system performance in three key areas: semantic matching accuracy suffers from misaligned spaces; retrieval stability is compromised by distributional drift; and long-tail queries perform poorly due to inadequate fine-grained semantic capture.

Therefore, resolving representational misalignment in dense retrieval is not only vital for improving traditional retrieval systems but also essential for ensuring high-quality semantic ID inputs in the era of generative recommendation systems. This paper delves into this core challenge and introduces a consistency-focused retrieval framework named SCI comprising two tightly integrated components: 1) **Symmetric Representation Alignment:** Introduces an innovative input-swapping mechanism—feeding query

samples into the item tower to generate item-view query representations, and item samples into the query tower to obtain query-view item representations. By applying a symmetric contrastive loss, the dual towers naturally converge toward a unified semantic space while preserving their individual encoding capabilities. This approach requires only additional forward passes during training, introduces no new parameters, and significantly improves representation quality. 2) **Consistent Indexing with dual-tower Synergy (CI):** Re-engineers retrieval path consistency. We propose a novel indexing strategy: when building a coarse-to-fine index (e.g., IVF-PQ), all item embeddings encoded by the query tower are used for coarse clustering, ensuring queries and centroids reside in the same semantic space. Then, within each cluster, the original item tower embeddings are used for residual quantization. This ensures the retrieval path remains aligned with the learning objective.

The proposed framework offers three key advantages: 1) **Systematic:** Ensures end-to-end consistency from training to retrieval via coordinated design of representation learning and indexing. 2) **Simple:** Only introduces input swapping during training without complex external modules. 3) **Engineering-Friendly:** Minimal training overhead, and indexing is fully compatible with industrial ANN libraries, supporting billion-scale deployment. To validate the framework, we performed comprehensive experiments on two large publicly available datasets and a real-world billion-scale e-Commerce data set. Offline evaluations demonstrated significant improvements in core metrics such as Recall and MAP. The main contributions of this work are summarized as follows:

- We propose a novel consistency-oriented retrieval framework that systematically addresses alignment issues across the entire pipeline—from representation learning to retrieval execution.
- We introduce Symmetric Representation Alignment (SymAligner), an efficient input-swapping mechanism for cross-tower alignment, and Consistent Indexing with dual-tower synergy (CI), a novel indexing architecture that incorporates query-side information into index construction.
- We provide extensive validations on large publicly and industrial datasets, offering a practical and scalable solution for optimizing large-scale dense retrieval systems.

## 2 Related Works

### 2.1 Representation Learning

The dual-tower model is the predominant architecture for large-scale dense retrieval due to its efficiency with pre-computable vectors for Approximate Nearest Neighbor (ANN) search [11, 21, 25, 32, 33]. However, its decoupled design inherently leads to a representation space misalignment between queries and items. Existing efforts to mitigate this, such as enhanced negative sampling [14, 30], late-interaction mechanisms [25, 27], or knowledge distillation from cross-attention models [4], often introduce significant scalability challenges, including increased inference latency or complex training procedures, limiting their practical deployment.

### 2.2 Approximate Retrieval

To achieve millisecond-level latency over billion-item corpora, ANN search [13] is essential and universally relies on a coarse-to-fine

hierarchical paradigm. This principle underpins clustering-based methods like IVF [24] and graph-based methods like HNSW [20], which first narrow the search space to a promising subset before performing fine-grained comparisons. Modern data-driven approaches, such as Semantic IDs, also learn a hierarchical discrete partitioning of the semantic space, effectively internalizing this coarse-to-fine structure. The performance of this entire retrieval pipeline, however, is fundamentally dependent on the quality and consistency of the initial vector representations.

### 2.3 Joint Index Optimization

The optimization of representation learning and index retrieval has traditionally been decoupled. Some research has explored joint optimization, which integrates index structures or quantization losses directly into model training [9, 34, 36, 39]. However, these methods are often computationally intensive and exhibit poor compatibility with highly optimized, standard ANN libraries. Consequently, the industry standard remains a decoupled approach for its engineering simplicity and stability. The central challenge, which this paper addresses, is to resolve the foundational representation space misalignment within this practical, decoupled framework, ensuring consistency between the learned representations and the downstream retrieval index.

## 3 Methodology

### 3.1 Overview

Our proposed framework, illustrated in Figure 2, addresses dual-tower retrieval limitations through an integrated pipeline comprising two synergistic components. The complete workflow operates as follows: during training, the **Symmetric Representation Alignment (SymmAligner)** component performs input swapping between query and item encoders, computes an alignment loss, and optimizes model parameters to eliminate representation anisotropy. During indexing, the **Consistent Indexing with Dual-Tower Synergy (CI)** component processes all items through the query encoder to build cluster centers, then applies enhanced quantization using embeddings from both towers. For retrieval, queries are encoded through the query encoder and efficiently searched using the unified index.

The framework offers crucial advantages: it requires no architectural changes, introduces minimal computational overhead, maintains compatibility with various ANN algorithms, and demonstrates universal applicability across different encoder architectures (BERT, ResNet, etc.) and multimodal scenarios (text-image, text-video retrieval). The tight integration between symmetric training and consistent indexing ensures representation compatibility while preserving the efficiency benefits of dual-tower architectures.

### 3.2 Symmetric Representation Alignment (SymmAligner)

The fundamental challenge of dual-tower models lies in the incompatible representation spaces learned by the query encoder  $f_q$  and item encoder  $f_i$  during independent optimization. This incompatibility causes even semantically related queries and items to have distant embedding vectors in the representation space. To overcome

this limitation, we propose a simple symmetric representation alignment method based on input swapping.

**3.2.1 Training Framework and Loss Formulation.** Our training framework builds upon the traditional dual-tower optimization pipeline while introducing a novel symmetric objective to enforce representation alignment. The standard approach relies on a triplet loss, which we refer to as the original loss ( $\mathcal{L}_{\text{original}}$ ), to ensure task-specific performance. For a given training sample  $(Q, I^+, I^-)$ , this loss is formulated as:

$$\mathcal{L}_{\text{original}}(\theta_q, \theta_i) = \mathbb{E}_{(Q, I^+, I^-)} [\max(0, \delta - S(f_q(Q), f_i(I^+)) + S(f_q(Q), f_i(I^-)))] \quad (1)$$

While effective for the primary retrieval task, this objective does not explicitly prevent the query and item encoders from learning incompatible, anisotropic representations.

To overcome this limitation, we introduce an innovative input-swapping mechanism. For each training sample, in addition to the standard embeddings, we compute a set of swapped embeddings. We feed the query  $Q$  into the item encoder to obtain an item-view query representation, denoted as  $\mathbf{v}_{q, \text{swap}} = f_i(Q)$ , and conversely, feed items  $I^+, I^-$  into the query encoder to obtain query-view item representations, denoted as  $\mathbf{v}_{i^+, \text{swap}} = f_q(I^+)$  and  $\mathbf{v}_{i^-, \text{swap}} = f_q(I^-)$ .

Based on these swapped representations, we construct a Swap Alignment Loss ( $\mathcal{L}_{\text{swap}}$ ) that mirrors the original objective:

$$\mathcal{L}_{\text{swap}}(\theta_q, \theta_i) = \mathbb{E}_{(Q, I^+, I^-)} [\max(0, \delta - S(\mathbf{v}_{q, \text{swap}}, \mathbf{v}_{i^+, \text{swap}}) + S(\mathbf{v}_{q, \text{swap}}, \mathbf{v}_{i^-, \text{swap}}))] \quad (2)$$

This loss function forces the model to maintain correct similarity relationships even when the encoders' roles are reversed. This symmetric constraint incentivizes both encoders to learn a shared, compatible representation space that preserves semantic consistency regardless of the input's origin.

The complete training objective, our total loss ( $\mathcal{L}_{\text{total}}$ ), combines both the standard retrieval objective and our novel alignment objective:

$$\mathcal{L}_{\text{total}}(\theta_q, \theta_i) = (1 - \lambda)\mathcal{L}_{\text{original}}(\theta_q, \theta_i) + \lambda\mathcal{L}_{\text{swap}}(\theta_q, \theta_i) \quad (3)$$

The hyperparameter  $\lambda$  controls the balance of alignment strength, typically set in the range [0.1, 1.0]. This symmetric training approach offers several notable advantages: it preserves the model architecture with only additional forward computation overhead; requires no additional training data; works with various encoder types and multimodal scenarios; and enables flexible alignment control through a simple hyperparameter adjustment.

**3.2.2 Gradient Analysis and Theoretical Foundations.** Understanding how the swap loss promotes representation alignment by providing complementary gradient paths is crucial for deeply appreciating the effectiveness of our method. By analyzing the gradient propagation mechanism, we can clearly see how the swap loss provides additional optimization signals for the dual-tower model.

For query tower parameters  $\theta_q$ , the total gradient  $\nabla_{\theta_q} \mathcal{L}_{\text{total}}$  synthesizes two distinct optimization paths:

**Original loss gradient path:**

$$\nabla_{\theta_q} \mathcal{L}_{\text{original}} \propto \mathbb{E} \left[ \left( -\nabla_{\theta_q} S(f_q(Q), f_i(I^+)) + \nabla_{\theta_q} S(f_q(Q), f_i(I^-)) \right) \right] \quad (4)$$

This path flows exclusively through the query tower's encoding of queries, training the query tower to become a specialized query encoder. It focuses on making query representations better interact

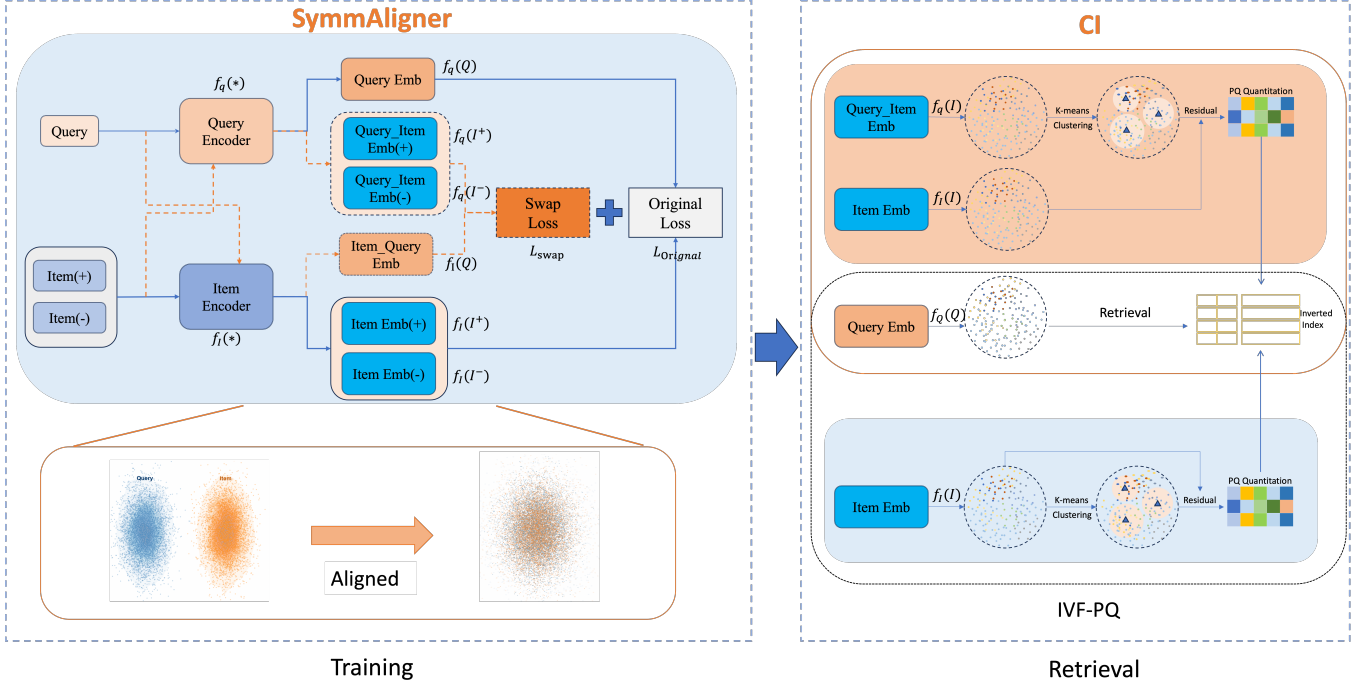


**Figure 2: The workflow of SCI: (a) Symmetric Representation Alignment (SymmAligner) via input swapping and joint optimization, (b) Consistent Indexing with Dual-Tower Synergy (CI) compared to traditional IVF-PQ, where CI uses the query encoder for unified representation with dual-tower enhancement.**

with item representations, but doesn't directly address the problem of representation space alignment.

#### Swap loss gradient path:

$$\nabla_{\theta_q} \mathcal{L}_{\text{swap}} \propto \mathbb{E} \left[ \left( -\nabla_{\theta_q} S(f_i(Q), f_q(I^+)) + \nabla_{\theta_q} S(f_i(Q), f_q(I^-)) \right) \right] \quad (5)$$

This innovative path flows through the query tower's encoding of items, forcing the query tower to also learn meaningful representations for items. This symmetric effect similarly applies to the item tower, creating a bidirectional optimization mechanism that compels both towers to learn a shared universal semantic mapping.

**3.2.3 Theoretical Foundations.** The swap loss mechanism provides theoretical guarantees for representation alignment through complementary gradient paths and space regularization.

**LEMMA 3.1 (GRADIENT LINEAR INDEPENDENCE).** *Under the condition that query and item distributions are not identical, the gradients  $\nabla_{\theta_q} \mathcal{L}_{\text{original}}$  and  $\nabla_{\theta_q} \mathcal{L}_{\text{swap}}$  are generally linearly independent. (Proof see Appendix B.1)*

**LEMMA 3.2 (REPRESENTATION ALIGNMENT).** *Minimizing  $\mathcal{L}_{\text{total}}$  implicitly minimizes the alignment error (Proof see Appendix B.2):*

$$\mathcal{A}(\theta_q, \theta_i) = \mathbb{E}_{Q, I} \left[ \left( S(f_q(Q), f_i(I)) - S(f_i(Q), f_q(I)) \right)^2 \right] \quad (6)$$

**LEMMA 3.3 (ANISOTROPY REDUCTION).** *The swap loss regularizes the embedding space, reducing anisotropy by enforcing compatible covariance structures (Proof see Appendix B.3):*

$$\text{Cov}(f_q(Q \cup I)) \approx \text{Cov}(f_i(Q \cup I)) \quad (7)$$

Collectively, these lemmas establish that our symmetric training approach addresses the core limitations of dual-tower architectures. Lemma 3.1 ensures non-redundant optimization signals, Lemma 3.2 guarantees representation space compatibility, and Lemma 3.3 enables effective nearest neighbor search by creating an isotropic embedding space. These theoretical properties form the foundation for our consistent indexing framework.

**3.2.4 Linear Model Analysis.** To ground our theoretical results in concrete mathematical intuition, we analyze a simplified single-layer linear dual-tower model.

Consider linear transformations  $f_q(Q) = W_q q$  and  $f_i(I) = W_i i$ . The total gradient reveals a symmetrization mechanism:

$$\frac{\partial \mathcal{L}_{\text{total}}}{\partial W_q} = W_i [\Delta i q^\top + \lambda q \Delta i^\top] \quad (8)$$

where  $\Delta i = i^- - i^+$ . This suggests the symmetrization operator:

$$M(q, \Delta i) = \frac{1}{2} (q \Delta i^\top + \Delta i q^\top) \quad (9)$$

**Collapse analysis** reveals that the swap loss provides meaningful signals except in degenerate cases: (1)  $\lambda = 0$  (no swap loss), (2)  $q \parallel \Delta i$  (vector parallelism), or (3) special orthogonal conditions. In practice, these conditions are rarely satisfied since queries and items typically exhibit different statistical properties. (Detailed analysis see Appendix B.6)

**Algorithm 1** Symmetric Representation Alignment (SymmAligner) Training

**Require:** Query encoder  $f_q$ , item encoder  $f_i$ , dataset  $\mathcal{D}$ , margin  $\delta$ , alignment weight  $\lambda$

**Ensure:** Aligned encoders  $f_q^*, f_i^*$

```

1: Initialize  $f_q, f_i$  with standard pretrained weights
2: for each training batch  $(Q, I^+, I^-)$  do
3:   // Compute standard embeddings and loss
4:    $\mathbf{v}_q \leftarrow f_q(Q); \mathbf{v}_{i^+} \leftarrow f_i(I^+); \mathbf{v}_{i^-} \leftarrow f_i(I^-)$ 
5:    $\mathcal{L}_{\text{original}} \leftarrow \max(0, \delta - S(\mathbf{v}_q, \mathbf{v}_{i^+}) + S(\mathbf{v}_q, \mathbf{v}_{i^-}))$ 
6:   // Compute swapped embeddings and loss
7:    $\mathbf{v}_{q,\text{swap}} \leftarrow f_i(Q); \mathbf{v}_{i^+,\text{swap}} \leftarrow f_q(I^+); \mathbf{v}_{i^-,\text{swap}} \leftarrow f_q(I^-)$ 
8:    $\mathcal{L}_{\text{swap}} \leftarrow \max(0, \delta - S(\mathbf{v}_{q,\text{swap}}, \mathbf{v}_{i^+,\text{swap}}) + S(\mathbf{v}_{q,\text{swap}}, \mathbf{v}_{i^-,\text{swap}}))$ 
9:   // Combined optimization
10:   $\mathcal{L}_{\text{total}} \leftarrow \mathcal{L}_{\text{original}} + \lambda \mathcal{L}_{\text{swap}}$ 
11:  Update  $\theta_q, \theta_i$  using  $\nabla \mathcal{L}_{\text{total}}$ 
12: end for
13: return  $f_q, f_i$ 

```

### 3.3 Consistent Indexing with Dual-Tower Synergy (CI)

Building upon the representation alignment achieved through SymmAligner, we introduce the **Consistent Indexing with Dual-Tower Synergy (CI)** framework to eliminate the distribution mismatch in traditional dual-tower retrieval.

Traditional dual-tower retrieval suffers from inherent inconsistency: queries and items are encoded through different towers, yet compared during retrieval. This can be formalized as:

$$\{I_1, \dots, I_k\} = \mathcal{A}(f_q(Q), \{f_i(I)\}_{I \in \mathcal{D}}) \quad (10)$$

where the ANN algorithm  $\mathcal{A}$  must bridge the gap between query space  $f_q$  and item space  $f_i$ .

Our solution leverages the aligned representations from SymmAligner to create a unified indexing scheme:

$$\{I_1, \dots, I_k\} = \mathcal{A} \left( \underbrace{f_q(Q)}_{\text{Coarse Structure}}, \underbrace{\{f_q(I)\}_{I \in \mathcal{D}}}_{\text{Fine Representation}}, \underbrace{\{f_i(I)\}_{I \in \mathcal{D}}}_{\text{Fine Representation}} \right) \quad (11)$$

The key innovation lies in assigning distinct roles to each tower: the query encoder defines the coarse index structure, while both towers contribute to fine-grained representations. This synergistic approach is enabled by the representation alignment (Lemma 3.2) and isotropy (Lemma 3.3) achieved through SymmAligner.

**3.3.1 Dual-Vector Strategy and IVF-PQ Implementation.** We implement this framework through a Dual-Vector Strategy that generates specialized embeddings for each item  $I \in \mathcal{D}$ :

$$\begin{aligned} \mathbf{e}_I^q &= f_q(I) \quad (\text{Structural Vector}) \\ \mathbf{e}_I^i &= f_i(I) \quad (\text{Representation Vector}) \end{aligned}$$

In the widely used IVF-PQ scheme, this strategy translates to two key steps:

**Algorithm 2** Consistent Indexing with Dual-Tower Synergy

**Require:** Trained encoders  $f_q, f_i$ , item collection  $\mathcal{D}$ , ANN algorithm  $\mathcal{A}$

**Ensure:** Consistent index for efficient retrieval

```

1: Index Construction Phase:
2: for each item  $I \in \mathcal{D}$  do
3:    $\mathbf{e}_I^q \leftarrow f_q(I)$  ▷ Structural vector
4:    $\mathbf{e}_I^i \leftarrow f_i(I)$  ▷ Representation vector
5: end for
6:  $\{\mathbf{c}_1, \dots, \mathbf{c}_K\} \leftarrow \text{k-means}(\{\mathbf{e}_I^q\}, K)$  ▷ Unified clustering
7: for each item  $I \in \mathcal{D}$  do
8:    $k(I) \leftarrow \arg \min_j \|\mathbf{e}_I^q - \mathbf{c}_j\|^2$  ▷ Cluster assignment in unified space
9:    $\mathbf{r}_I \leftarrow \mathbf{e}_I^i - \mathbf{c}_{k(I)}$  ▷ Hybrid-space residual computation
10: end for
11:  $\text{index} \leftarrow \mathcal{A}.\text{build}(\{\mathbf{e}_I^q, \mathbf{r}_I : I \in \mathcal{D}\})$  ▷ Algorithm-specific construction
12: Retrieval Phase:
13:  $\mathbf{e}_Q \leftarrow f_q(Q)$  ▷ Query encoding in unified space
14:  $\{I_1, \dots, I_k\} \leftarrow \mathcal{A}.\text{search}(\mathbf{e}_Q, \text{index}, k)$  ▷ Consistent retrieval
15: return  $\{I_1, \dots, I_k\}$ 

```

(1) **Unified Clustering:** Cluster centers are computed exclusively from structural vectors to ensure query-space consistency:

$$\{\mathbf{c}_1, \dots, \mathbf{c}_K\} = \text{k-means}(\{\mathbf{e}_I^q\}_{I \in \mathcal{D}}, K) \quad (12)$$

(2) **Hybrid-Space Residual Computation:** Items are assigned to clusters based on structural vectors, but residuals are computed using representation vectors:

$$k(I) = \arg \min_j \|\mathbf{e}_I^q - \mathbf{c}_j\|^2 \quad (13)$$

$$\text{s.t. } \mathbf{r}_I = \mathbf{e}_I^i - \mathbf{c}_{k(I)} \quad (14)$$

This hybrid approach leverages the strengths of both towers: the structural vectors ensure consistency with query encoding, while the representation vectors potentially capture richer item-specific information for accurate quantization. The mathematical soundness of cross-space residual computation is guaranteed by the encoder equivalence ( $f_q(I) \approx f_i(I)$ ) established through SymmAligner.

**3.3.2 Algorithm-Agnostic Generalization.** The power of the Dual-Vector Strategy lies in its generality. While the IVF-PQ implementation showcases its effectiveness, the principle of separating coarse structure from fine representation is broadly applicable to other major ANN families:

- **Quantization methods (IVF-FLAT, IVF-OPQ):** Use  $\mathbf{e}_I^q$  for coarse clustering and the hybrid-space  $\mathbf{r}_I$  for product quantization.
- **Graph methods (HNSW):** Build the graph on the structural vectors  $\{\mathbf{e}_I^q\}$  to ensure consistent routing, while final distance calculations can optionally use the high-fidelity representation vectors  $\mathbf{e}_I^i$  for refinement.

**3.3.3 Theoretical Guarantees for Indexing Consistency.** The SymmAligner component provides the theoretical foundation for consistent indexing through representation alignment.

**THEOREM 3.4 (RETRIEVAL CONSISTENCY).** *Using item representations from the query tower,  $\{f_q(I)\}$ , for index construction aligns the ANN search objective with the model’s true objective.*

**COROLLARY 3.5 (ENHANCED RETRIEVAL WITH DUAL-TOWER SYNERGY).** *The dual-tower enhanced implementation maintains retrieval consistency while providing improved quantization accuracy through residual computation.*

These results establish that our indexing framework fundamentally solves the distribution mismatch problem in dual-tower retrieval. Theorem 3.4 guarantees that approximate nearest neighbor search accurately reflects true semantic similarity, while the corollary demonstrates that our dual-tower enhancement maintains this consistency while improving quantization quality through hybrid-space residual computation.

### 3.4 Complexity Analysis

We analyze the computational complexity of our framework compared to conventional dual-tower models, with key results summarized in Table 5. The proposed framework introduces carefully balanced trade-offs:

- **Training:** Complexity increases from  $O(F + B)$  to  $O(2F + B)$  due to the additional forward passes for input swapping, though this is partially offset by faster convergence.
- **Index Construction:** Offline complexity increases from  $O(N \cdot T_i)$  to  $O(N \cdot (T_q + T_i))$  as we compute both structural and representation vectors.
- **Online Service:** Crucially, all inference metrics remain identical to conventional approaches, preserving real-time performance with  $O(D + K \cdot D + n_{\text{probe}} \cdot \frac{N}{K} \cdot M)$  complexity.

This design accepts moderate offline costs to achieve significant improvements in representation quality and retrieval consistency, while maintaining deployment efficiency for industrial-scale systems.

## 4 Experiments

In this section, we conduct comprehensive experiments to answer three central research questions (RQs):

- **RQ1(Overall Performance):** Does our SymmAligner and CI framework achieve state-of-the-art performance against baselines?
- **RQ2(Component-wise Effectiveness):** What are the individual contributions of SymmAligner and CI, and how do they address the core issues of representation and index inconsistency?
- **RQ3(Robustness and Sensitivity):** How robust is our framework to variations in key hyperparameters (e.g., alignment weight  $\lambda$ )?

### 4.1 Datasets and Metrics

Our evaluation is grounded in two settings: a standard public benchmark and a large-scale industrial environment.

- **MS MARCO (MS300k) [1]:** A widely-used public benchmark for document retrieval [5, 17, 28, 37]. We follow the preprocessing protocol from [38] for URL-based deduplication, using its train/dev sets for our experiments.

- **Industrial E-commerce Dataset:** A proprietary dataset of 10 million user query-item click interactions from a large e-commerce platform, with a corpus of 1 million items. This dataset reflects the challenges of a real-world production environment.

For MS MARCO, we report standard metrics [5, 6, 26, 37]: Mean Reciprocal Rank (MRR@K) and Recall@K. For the industrial dataset, we focus on metrics crucial for large-scale candidate generation: Precision@K, Recall@K, and NDCG@K.

### 4.2 Baselines

Our comparative analysis includes three categories of retrieval methods.

- **Sparse retrieval:** BM25, and advanced learned sparse models like UniCOIL [18] and SPLADEv2 [10].
- **Standard dense retrieval:** DPR [14], ANCE [31], and critically, our own **Bert2Tower**, which uses the BERT backbone and training setup as our method (sans SymmAligner and CI) to ensure a fair and direct comparison.
- **Enhanced dense retrieval:** GTR-Base [22], a pre-trained generalizable T5-based dense retrievers.

Our work focuses on enhancing the standard, pre-computation dual-tower paradigm, which is fundamental to industrial-scale, low-latency retrieval systems. We therefore do not directly compare against methods that alter this paradigm. Late-interaction models (e.g., ColBERT [15]) sacrifice pre-computation efficiency for higher-cost runtime interactions. Knowledge distillation methods rely on computationally expensive teacher models (e.g., Cross-Encoders), whereas our approach is self-contained. Joint optimization methods typically focus on minimizing quantization loss but do not address the precedent, more fundamental problem of representation space misalignment that our framework targets.

Note that, we did not employ a parameter-sharing architecture due to the inherent data heterogeneity (e.g., text queries vs. multimodal items) and architectural asymmetry (a lightweight online query tower vs. a complex offline item tower). This dual conflict induces a "seesaw effect," which degrades the representation quality for both sides. We confirmed this empirically on an industrial dataset, where our parameter-sharing model, Bert2Tower-Shared, showed a drop in performance.

### 4.3 Implementation Details

All dense retrievers are built upon the BERT encoder architecture [7]. We use the AdamW optimizer with a constant learning rate  $1 \times 10^{-5}$ , preceded by a linear warmup phase. The embedding dimension is 768. For SymmAligner, the alignment weight  $\lambda$  was set to 0.3 based on a grid search on a validation set. For ANN indexing, we use IVF-PQ[13] with  $nlist = 4096$ ,  $nprobe = 64$ , and  $M = 64$  (64-byte codes), unless stated otherwise.

### 4.4 Overall Results (RQ1 and RQ3)

Table 1 presents the main results of our framework against various baselines on the MS MARCO dataset, including a detailed ablation study on the SymmAligner alignment weight,  $\lambda$ . The results validate our framework’s effectiveness through three key findings.

**Table 1: Main results on the MS MARCO (MS300K) dataset. Bert2Tower is our baseline dual-tower model. SCI (Bert2Tower+SymmAligner) is the upper bound of our SymmAligner-trained model with exact search. Proposed ( $\lambda=...$ ) are our full practical frameworks (SCI) with different alignment weights.**

Category	Method	MS MARCO (MS300K)				
		MRR@10	MRR@100	Recall@1	Recall@10	Recall@100
Sparse	BM25	0.248	0.255	0.186	0.391	0.573
	UniCOIL	0.425	0.435	0.284	0.766	0.951
	SPLADEv2	0.443	0.452	0.328	0.779	0.956
Dense(Brute-Force)	DPR	0.424	0.433	0.271	0.764	0.948
	ANCE	0.451	0.455	0.299	0.785	0.953
	GTR-Base	0.576	0.581	0.471	0.785	0.912
	Bert2Tower	0.480	0.488	0.372	0.714	0.893
	<b>SCI (Bert2Tower+ SymmAligner)</b>	<b>0.496</b>	<b>0.504</b>	<b>0.383</b>	<b>0.737</b>	<b>0.908</b>
Dense(IVF-Flat)	Bert2Tower	0.408	0.414	0.318	0.603	0.750
	SCI ( $\lambda = 0.1$ )	0.369	0.374	0.287	0.545	0.674
	SCI ( $\lambda = 0.2$ )	0.400	0.407	0.316	0.580	0.721
	<b>SCI (<math>\lambda = 0.3</math>)</b>	<b>0.448</b>	<b>0.455</b>	<b>0.350</b>	<b>0.657</b>	<b>0.805</b>
	SCI ( $\lambda = 0.4$ )	0.420	0.426	0.324	0.620	0.756
	SCI ( $\lambda = 0.5$ )	0.393	0.399	0.303	0.588	0.717

First, our full, practical framework demonstrates a significant performance advantage over the comparable baseline. Our best model, **SCI** ( $\lambda = 0.3$ ), achieves an MRR@10 of **0.448**, which is a substantial **9.9% relative improvement** over the **Bert2Tower** baseline (0.408). This direct, apples-to-apples comparison on indexed systems confirms that our end-to-end consistency-oriented approach (SCI) effectively resolves the bottlenecks in standard dual-tower retrieval, leading to superior ranking quality.

Second, the results clearly delineate the two-stage contribution of our framework. The brute-force evaluation of **SCI (Only SymmAligner)** (MRR@10=0.496) shows a marked improvement over the **Bert2Tower** counterpart (0.480), confirming that SymmAligner successfully creates a higher-quality representation space. While ANN indexing inevitably introduces a performance gap, our final model (MRR@10=0.448) successfully preserves a large portion of the gains established by SymmAligner, demonstrating the crucial role of CI in translating theoretical representation quality into practical performance.

Finally, the ablation on the alignment weight  $\lambda$  reveals a non-trivial trade-off and offers important insights. Performance steadily improves as  $\lambda$  increases from 0.1 to 0.3, peaking at our best model. However, as  $\lambda$  increases further to 0.5, performance begins to decline. This demonstrates that while the symmetric alignment signal from  $\mathcal{L}_{\text{swap}}$  is critical, an excessive alignment constraint can start to interfere with the primary retrieval objective of  $\mathcal{L}_{\text{original}}$ . The existence of an optimal "sweet spot" at  $\lambda = 0.3$  empirically validates our approach of balancing these two loss components, providing a clear and practical methodology for optimizing consistency in dual-tower models.

#### 4.5 Analysis on SymmAligner (RQ2)

As shown in Table 2, the baseline model achieves a mean similarity of 0.615 for ground-truth pairs. Our SymmAligner-enhanced model

**Table 2: Cosine similarity for ground-truth query-item pairs on the MS MARCO test set.**

Statistic Metric	Bert2Tower	SymmAligner
Mean Similarity	0.615	<b>0.672</b>
Median Similarity	0.625	<b>0.684</b>
Minimum Similarity	0.232	<b>0.364</b>
Maximum Similarity	0.783	<b>0.830</b>
Std. Deviation	0.066	<b>0.065</b>

increases this value to **0.672**, a relative improvement of 9.3%. This quantitative increase in average similarity provides direct empirical validation for **Lemma 3.2**, demonstrating a more effective and consistent alignment of positive pairs.

Of particular significance is the change in the minimum similarity, which increases by over 50% from 0.232 to **0.364**. The baseline's lower value indicates the presence of challenging positive pairs that are mapped to geometrically distant regions in the embedding space. The substantial improvement in this worst-case alignment suggests a more robust and uniform semantic manifold. By significantly improving the scores of these hardest pairs, SymmAligner mitigates the detrimental effects of representation inconsistencies—a key goal related to **Lemma 3.3**—and reduces the risk of catastrophic ranking failures.

#### 4.6 Analysis on CI (RQ2)

We validate CI by analyzing its performance under varying search scopes controlled by nprobe (Table 3). The nprobe parameter, representing the computational cost of the coarse search, allows for a direct evaluation of the index's accuracy and efficiency.

**Table 3: Performance comparison with different nprobe values.**

Method		Precision			Recall			MRR			NDCG		
		@1	@10	@100	@1	@10	@100	@1	@10	@100	@1	@10	@100
nprobe=1	Bert2Tower	0.1348	0.0277	0.0035	0.1348	0.2767	0.3476	0.1348	0.1771	0.1807	0.1348	0.0528	0.0571
	SCI( $\lambda = 0.3$ )	0.1662	0.0327	0.0039	0.1662	0.3268	0.3929	0.1662	0.2157	0.2189	0.1662	0.0637	0.0677
nprobe=8	Bert2Tower	0.2634	0.0502	0.0062	0.2634	0.5020	0.6241	0.2634	0.3372	0.3429	0.2634	0.0988	0.1060
	SCI( $\lambda = 0.3$ )	0.2770	0.0530	0.0065	0.2770	0.5300	0.6478	0.2770	0.3560	0.3613	0.2770	0.1043	0.1112
nprobe=16	Bert2Tower	0.2952	0.0556	0.0069	0.2952	0.5564	0.6933	0.2952	0.3766	0.3829	0.2952	0.1101	0.1180
	SCI( $\lambda = 0.3$ )	0.3054	0.0578	0.0071	0.3054	0.5782	0.7083	0.3054	0.3921	0.3980	0.3054	0.1145	0.1220
nprobe=32	Bert2Tower	0.3181	0.0603	0.0075	0.3181	0.6030	0.7501	0.3181	0.4077	0.4144	0.3181	0.1192	0.1277
	SCI( $\lambda = 0.3$ )	0.3291	0.0617	0.0076	0.3291	0.6171	0.7575	0.3291	0.4202	0.4265	0.3291	0.1225	0.1306
nprobe=64	Bert2Tower	0.3403	0.0641	0.0080	0.3403	0.6410	0.7968	0.3403	0.4353	0.4423	0.3403	0.1270	0.1360
	SCI( $\lambda = 0.3$ )	0.3501	0.0657	0.0081	0.3501	0.6568	0.8053	0.3501	0.4480	0.4547	0.3501	0.1305	0.1391

**Table 4: Performance on the industrial dataset. The top section shows brute-force search results. The bottom section shows results with an IVF-PQ index.**

Category	Method	Precision			Recall			MRR			NDCG		
		@10	@100	@1000	@10	@100	@1000	@10	@100	@1000	@10	@100	@1000
Dense (Brute-Force)	Bert2Tower-Shared	0.0579	0.0114	0.0014	0.4286	0.7997	0.9664	0.2268	0.2412	0.2420	0.2657	0.3510	0.3746
	Bert2Tower	0.0588	0.0115	0.0014	0.4344	0.8056	0.9683	0.2367	0.2514	0.2521	0.2739	0.3594	0.3823
	SCI w/o CI	<b>0.0594</b>	<b>0.0115</b>	<b>0.0014</b>	<b>0.4389</b>	<b>0.8065</b>	<b>0.9678</b>	<b>0.2373</b>	<b>0.2516</b>	<b>0.2523</b>	<b>0.2755</b>	<b>0.3600</b>	<b>0.3828</b>
Dense (IVF-PQ)	Bert2Tower	0.0322	0.0085	0.0013	0.2378	0.5984	0.8881	0.1182	0.1317	0.1329	0.1385	0.2181	0.2582
	SCI ( $\lambda = 0.1$ )	0.0322	0.0083	0.0012	0.2392	0.5814	0.8627	0.1234	0.1362	0.1374	0.1430	0.2188	0.2575
	<b>SCI</b> ( $\lambda = 0.3$ )	<b>0.0368</b>	<b>0.0089</b>	0.0013	<b>0.2718</b>	<b>0.6222</b>	0.8793	<b>0.1360</b>	<b>0.1493</b>	<b>0.1503</b>	<b>0.1603</b>	<b>0.2384</b>	<b>0.2740</b>
	SCI ( $\lambda = 0.5$ )	0.0229	0.0073	0.0012	0.1706	0.5162	0.8571	0.0798	0.0922	0.0937	0.0962	0.1705	0.2177

As the results show, at a minimal search scope of  $nprobe=1$ , our method improves Recall@10 by 18% relative to the traditional index (Bert2Tower). This demonstrates a more accurate coarse-grained lookup, as the initial cluster searched in the CI index is more likely to contain relevant items. This improved accuracy translates to greater overall search efficiency. For example, our CI at  $nprobe=8$  achieves an MRR@100 of 0.3613, a value comparable to the baseline which requires a larger search scope of  $nprobe=16$  to reach a similar score of 0.3829. This indicates that CI can achieve a similar level of ranking quality with approximately half the computational cost. The ability to attain higher accuracy with a smaller search scope empirically validates **Theorem 3.4**, confirming that our consistent indexing creates a more effective and efficient retrieval path.

#### 4.7 Results on Industrial-Scale Data

To validate our framework’s practical value and scalability, we present results from a large-scale industrial e-commerce dataset in Table 4. The baseline results starkly illustrate the core challenge addressed by this paper: a massive performance gap exists between the model’s brute-force potential (Bert2Tower, R@100=0.8056) and its practical performance after applying a standard IVF-PQ index (Bert2Tower, R@100=0.5984). This gap underscores the severe performance degradation caused by representation and indexing inconsistencies in a real-world production system.

Our consistency-oriented framework is designed to bridge this gap. Our full system, SCI ( $\lambda = 0.3$ ), significantly improves upon the indexed baseline, achieving a **4.0% relative gain in Recall@100**

and, more critically, a **9.3% relative gain in NDCG@100**. The substantial NDCG lift provides a deeper insight that corroborates our findings on the public benchmark: our framework not only retrieves more relevant items but also ranks them more accurately at the top. This is the direct empirical outcome of our systematic, two-part solution. SymmAligner first creates a more robust representation space (evidenced by the consistent gains of SCI w/o CI in the brute-force evaluation), and CI then ensures this improved semantic structure is preserved during the coarse-to-fine ANN search, as validated by our  $nprobe$  analysis. The results also reveal an optimal alignment strength ( $\lambda = 0.3$ ), offering practical guidance. Ultimately, the industrial data provides strong evidence that our end-to-end consistency framework is highly effective at translating a model’s theoretical potential into tangible real-world performance.

## 5 Conclusion

In this paper, we mitigate the problem of representational and indexing inconsistency in dual-tower dense retrieval systems, a critical bottleneck for both traditional and emerging generative recommendation paradigms. We introduce a novel consistency-oriented framework featuring two synergistic components: Symmetric Representation Alignment (SymmAligner) to forge a unified, isotropic semantic space, and Consistent Indexing with dual-tower synergy (CI) to construct a consistent retrieval index. Extensive experiments on public benchmarks and a billion-scale industrial dataset validate that our integrated approach significantly improves retrieval

performance by systematically eliminating the mismatch between training and inference.

## References

- [1] Payal Bajaj, Daniel Campos, Nick Craswell, Li Deng, Jianfeng Gao, Xiaodong Liu, Rangan Majumder, Andrew McNamara, Bhaskar Mitra, Tri Nguyen, Mir Rosenberg, Xia Song, Alina Stoica, Saurabh Tiwary, and Tong Wang. 2018. MS MARCO: A Human Generated MACHine Reading COmprehension Dataset. arXiv:1611.09268 [cs.CL] <https://arxiv.org/abs/1611.09268>
- [2] Christopher F Barnes, Syed A Rizvi, and Nasser M Nasrabadi. 1996. Advances in residual vector quantization: A review. *IEEE transactions on image processing* 5, 2 (1996), 226–262.
- [3] Qi Chen, Bing Zhao, Haidong Wang, Mingqin Li, Chuanjie Liu, Zengzhong Li, Mao Yang, and Jingdong Wang. 2021. Spann: Highly-efficient billion-scale approximate nearest neighborhood search. *Advances in Neural Information Processing Systems* 34 (2021), 5199–5212.
- [4] Xilun Chen, Kushal Lakhotia, Barlas Oğuz, Anchit Gupta, Patrick Lewis, Stan Peshterliev, Yashar Mehdad, Sonal Gupta, and Wen-tau Yih. 2021. Salient phrase aware dense retrieval: Can a dense retriever imitate a sparse one? *arXiv preprint arXiv:2110.06918* (2021).
- [5] Jiehan Cheng, Zhicheng Dou, Yutao Zhu, and Xiaoxi Li. 2025. Descriptive and Discriminative Document Identifiers for Generative Retrieval. In *Proceedings of the AAAI Conference on Artificial Intelligence*, Vol. 39. 11518–11526.
- [6] Jiehan Cheng, Zhicheng Dou, Yutao Zhu, and Xiaoxi Li. 2025. Descriptive and Discriminative Document Identifiers for Generative Retrieval. In *Proceedings of the AAAI Conference on Artificial Intelligence*, Vol. 39. 11518–11526.
- [7] Jacob Devlin, Ming-Wei Chang, Kenton Lee, and Kristina Toutanova. 2019. Bert: Pre-training of deep bidirectional transformers for language understanding. In *Proceedings of the 2019 conference of the North American chapter of the association for computational linguistics: human language technologies, volume 1 (long and short papers)*. 4171–4186.
- [8] Qian Dong, Yiding Liu, Suqi Cheng, Shuaiqiang Wang, Zhicheng Cheng, Shuzi Niu, and Dawei Yin. 2022. Incorporating explicit knowledge in pre-trained language models for passage re-ranking. In *Proceedings of the 45th International ACM SIGIR Conference on Research and Development in Information Retrieval*. 1490–1501.
- [9] Yan Fang, Jingtao Zhan, Yiqun Liu, Jiaxin Mao, Min Zhang, and Shaoping Ma. 2022. Joint optimization of multi-vector representation with product quantization. In *CCF International Conference on Natural Language Processing and Chinese Computing*. Springer, 631–642.
- [10] Thibault Formal, Carlos Lassance, Benjamin Piwowarski, and Stéphane Clinchant. 2021. SPLADE v2: Sparse lexical and expansion model for information retrieval. *arXiv preprint arXiv:2109.10086* (2021).
- [11] Po-Sen Huang, Xiaodong He, Jianfeng Gao, Li Deng, Alex Acero, and Larry Heck. 2013. Learning deep structured semantic models for web search using clickthrough data. In *Proceedings of the 22nd ACM international conference on Information & Knowledge Management*. 2333–2338.
- [12] Herve Jegou, Matthijs Douze, and Cordelia Schmid. 2010. Product quantization for nearest neighbor search. *IEEE transactions on pattern analysis and machine intelligence* 33, 1 (2010), 117–128.
- [13] Jeff Johnson, Matthijs Douze, and Hervé Jégou. 2019. Billion-scale similarity search with GPUs. *IEEE Transactions on Big Data* 7, 3 (2019), 535–547.
- [14] Vladimir Karpukhin, Barlas Oğuz, Sewon Min, Patrick SH Lewis, Ledell Wu, Sergey Edunov, Danqi Chen, and Wen-tau Yih. 2020. Dense Passage Retrieval for Open-Domain Question Answering. In *EMNLP (1)*. 6769–6781.
- [15] Omar Khattab and Matei Zaharia. 2020. Colbert: Efficient and effective passage search via contextualized late interaction over bert. In *Proceedings of the 43rd International ACM SIGIR conference on research and development in Information Retrieval*. 39–48.
- [16] Zhirui Kuai, Zuxu Chen, Huimu Wang, Mingming Li, Dadong Miao, Binbin Wang, Xusong Chen, Li Kuang, Yuxing Han, Jiaxing Wang, et al. 2024. Breaking the Hourglass Phenomenon of Residual Quantization: Enhancing the Upper Bound of Generative Retrieval. *arXiv preprint arXiv:2407.21488* (2024).
- [17] Yongqi Li, Nan Yang, Liang Wang, Furu Wei, and Wenjie Li. 2023. Multiview identifiers enhanced generative retrieval. *arXiv preprint arXiv:2305.16675* (2023).
- [18] Jimmy Lin and Xueguang Ma. 2021. A few brief notes on deepimpact, coil, and a conceptual framework for information retrieval techniques. *arXiv preprint arXiv:2106.14807* (2021).
- [19] Sheng-Chieh Lin, Jheng-Hong Yang, and Jimmy Lin. 2020. Distilling dense representations for ranking using tightly-coupled teachers. *arXiv preprint arXiv:2010.11386* (2020).
- [20] Yu A Malkov and Dmitry A Yashunin. 2018. Efficient and robust approximate nearest neighbor search using hierarchical navigable small world graphs. *IEEE transactions on pattern analysis and machine intelligence* 42, 4 (2018), 824–836.
- [21] Kelong Mao, Jieming Zhu, Jinpeng Wang, Quanyu Dai, Zhenhua Dong, Xi Xiao, and Xiuqiang He. 2021. SimpleX: A simple and strong baseline for collaborative filtering. In *Proceedings of the 30th ACM international conference on information & knowledge management*. 1243–1252.
- [22] Jianmo Ni, Chen Qu, Jing Lu, Zhuyun Dai, Gustavo Hernandez Abrego, Ji Ma, Vincent Y Zhao, Yi Luan, Keith B Hall, Ming-Wei Chang, et al. 2021. Large dual encoders are generalizable retrievers. *arXiv preprint arXiv:2112.07899* (2021).
- [23] Shashank Rajput, Nikhil Mehta, Anima Singh, Raghunandan Hulikal Keshavan, Trung Vu, Lukasz Heldt, Lichan Hong, Yi Tay, Vinh Tran, Jonah Samost, et al. 2023. Recommender systems with generative retrieval. *Advances in Neural Information Processing Systems* 36 (2023), 10299–10315.
- [24] Sivic and Zisserman. 2003. Video Google: A text retrieval approach to object matching in videos. In *Proceedings ninth IEEE international conference on computer vision*. IEEE, 1470–1477.
- [25] Liangcai Su, Fan Yan, Jieming Zhu, Xi Xiao, Haoyi Duan, Zhou Zhao, Zhenhua Dong, and Ruiming Tang. 2023. Beyond two-tower matching: learning sparse retrievable cross-interactions for recommendation. In *Proceedings of the 46th international ACM SIGIR conference on research and development in information retrieval*. 548–557.
- [26] Yi Tay, Vinh Tran, Mostafa Dehghani, Jianmo Ni, Dara Bahri, Harsh Mehta, Zhen Qin, Kai Hui, Zhe Zhao, Jai Gupta, et al. 2022. Transformer memory as a differentiable search index. *Advances in Neural Information Processing Systems* 35 (2022), 21831–21843.
- [27] Yihan Wang, Fei Xiong, Zhixin Han, Qi Song, Kaiqiao Zhan, and Ben Wang. 2025. Unleashing the Potential of Two-Tower Models: Diffusion-Based Cross-Interaction for Large-Scale Matching. In *Proceedings of the ACM on Web Conference 2025*. 304–312.
- [28] Zihan Wang, Yujia Zhou, Yiteng Tu, and Zhicheng Dou. 2023. NOVO: Learnable and Interpretable Document Identifiers for Model-Based IR. In *Proceedings of the 32nd ACM International Conference on Information and Knowledge Management (Birmingham, United Kingdom) (CIKM '23)*. Association for Computing Machinery, New York, NY, USA, 2656–2665. doi:10.1145/3583780.3614993
- [29] Xiaohui Xie, Qian Dong, Bingning Wang, Feiyang Lv, Ting Yao, Weinan Gan, Zhijing Wu, Xiangsheng Li, Haitao Li, Yiqun Liu, et al. 2023. T2ranking: A large-scale chinese benchmark for passage ranking. In *Proceedings of the 46th International ACM SIGIR Conference on Research and Development in Information Retrieval*. 2681–2690.
- [30] Lee Xiong, Chenyan Xiong, Ye Li, Kwok-Fung Tang, Jialin Liu, Paul Bennett, Junaid Ahmed, and Arnold Overwijk. 2020. Approximate nearest neighbor negative contrastive learning for dense text retrieval. *arXiv preprint arXiv:2007.00808* (2020).
- [31] Lee Xiong, Chenyan Xiong, Ye Li, Kwok-Fung Tang, Jialin Liu, Paul Bennett, Junaid Ahmed, and Arnold Overwijk. 2020. Approximate nearest neighbor negative contrastive learning for dense text retrieval. *arXiv preprint arXiv:2007.00808* (2020).
- [32] Ji Yang, Xinyang Yi, Derek Zhiyuan Cheng, Lichan Hong, Yang Li, Simon Xiaoming Wang, Taibai Xu, and Ed H Chi. 2020. Mixed negative sampling for learning two-tower neural networks in recommendations. In *Companion proceedings of the web conference 2020*. 441–447.
- [33] Yantao Yu, Weipeng Wang, Zhoutian Feng, and Daiyue Xue. 2021. A dual augmented two-tower model for online large-scale recommendation. *DLP-KDD* (2021).
- [34] Jingtao Zhan, Jiaxin Mao, Yiqun Liu, Jiafeng Guo, Min Zhang, and Shaoping Ma. 2021. Jointly optimizing query encoder and product quantization to improve retrieval performance. In *Proceedings of the 30th ACM International Conference on Information & Knowledge Management*. 2487–2496.
- [35] Jingtao Zhan, Jiaxin Mao, Yiqun Liu, Jiafeng Guo, Min Zhang, and Shaoping Ma. 2021. Optimizing dense retrieval model training with hard negatives. In *Proceedings of the 44th international ACM SIGIR conference on research and development in information retrieval*. 1503–1512.
- [36] Jingtao Zhan, Jiaxin Mao, Yiqun Liu, Jiafeng Guo, Min Zhang, and Shaoping Ma. 2022. Learning discrete representations via constrained clustering for effective and efficient dense retrieval. In *Proceedings of the Fifteenth ACM International Conference on Web Search and Data Mining*. 1328–1336.
- [37] Peitian Zhang, Zheng Liu, Yujia Zhou, Zhicheng Dou, Fangchao Liu, and Zhao Cao. 2024. Generative Retrieval via Term Set Generation. In *Proceedings of the 47th International ACM SIGIR Conference on Research and Development in Information Retrieval (Washington DC, USA) (SIGIR '24)*. Association for Computing Machinery, New York, NY, USA, 458–468. doi:10.1145/3626772.3657797
- [38] Yujia Zhou, Jing Yao, Zhicheng Dou, Ledell Wu, Peitian Zhang, and Ji-Rong Wen. 2022. Ultron: An ultimate retriever on corpus with a model-based indexer. *arXiv preprint arXiv:2208.09257* (2022).
- [39] Han Zhu, Xiang Li, Pengye Zhang, Guozheng Li, Jie He, Han Li, and Kun Gai. 2018. Learning tree-based deep model for recommender systems. In *Proceedings of the 24th ACM SIGKDD international conference on knowledge discovery & data mining*. 1079–1088.

Table 5: Complexity Comparison Analysis

Dimension	Conventional Two-Tower	Proposed Method
Index and Retrieval	$\{I_1, \dots, I_k\} = \mathcal{A}(f_q(Q), \{f_i(I)\}_{I \in \mathcal{D}})$	$\{I_1, \dots, I_k\} = \mathcal{A}\left(f_q(Q); \underbrace{\{f_q(I)\}_{I \in \mathcal{D}}}_{\text{Coarse Structure}}, \underbrace{\{f_i(I)\}_{I \in \mathcal{D}}}_{\text{Fine Representation}}\right)$
Training Complexity	$O(F + B)$	$O(2F + B)$
Index Construction	$O(N \cdot T_i)$	$O(N \cdot (T_q + T_i))$
Index Storage	$O(KD + MK^*D^* + NM)$	Identical
Online Inference	$O(D + K \cdot D + n_{\text{probe}} \cdot \frac{N}{K} \cdot M)$	Identical
Memory Consumption	$O(P + M_{\text{Index}})$	Identical

## A Complexity Table

## B Proofs of Theoretical Results

### B.1 Proof of Lemma 3.1

PROOF. Let  $J_q(X) = \nabla_{\theta_q} f_q(X)$  be the Jacobian of the query tower. The gradients are expectations over Jacobians evaluated at different data distributions:

$$\begin{aligned} \nabla_{\theta_q} \mathcal{L}_{\text{original}} &\propto \mathbb{E}_{Q,I} [J_q(Q)^\top \cdot g_1(f_q(Q), f_i(I))] \\ \nabla_{\theta_q} \mathcal{L}_{\text{swap}} &\propto \mathbb{E}_{Q,I} [J_q(I)^\top \cdot g_2(f_i(Q), f_q(I))] \end{aligned}$$

where  $g_1$  and  $g_2$  are different gradient functions derived from the loss formulations.

Since the expectations are taken over Jacobians corresponding to inputs from different distributions ( $Q$  vs.  $I$ ), and assuming query and item distributions are not identical, the resulting gradient vectors are not scalar multiples of each other. This ensures  $\mathcal{L}_{\text{swap}}$  provides complementary, non-redundant optimization signals.

More formally, if we assume  $\nabla_{\theta_q} \mathcal{L}_{\text{swap}} = \alpha \nabla_{\theta_q} \mathcal{L}_{\text{original}}$  for some scalar  $\alpha$ , this would imply that the Jacobians evaluated at query and item inputs are linearly dependent, which contradicts the assumption that query and item distributions are distinct and the encoders are sufficiently expressive.  $\square$

### B.2 Proof of Lemma 3.2

PROOF. At an optimal parameterization  $\theta^*$ , both loss components are minimized, i.e.,  $\mathcal{L}_{\text{original}}(\theta^*) \rightarrow 0$  and  $\mathcal{L}_{\text{swap}}(\theta^*) \rightarrow 0$ . This implies that for any given triplet, the following conditions must hold:

$$S(f_q(Q), f_i(I^+)) - S(f_q(Q), f_i(I^-)) \geq \delta \quad (15)$$

$$S(f_i(Q), f_q(I^+)) - S(f_i(Q), f_q(I^-)) \geq \delta \quad (16)$$

Let  $\Delta_{\text{orig}}$  and  $\Delta_{\text{swap}}$  be the score differences in (15) and (16) respectively. The optimization encourages both  $\Delta_{\text{orig}}$  and  $\Delta_{\text{swap}}$  to be close to the margin  $\delta$ . Consequently, their difference is driven towards zero in expectation:

$$\mathbb{E}[\Delta_{\text{orig}} - \Delta_{\text{swap}}] \rightarrow 0 \quad (17)$$

Expanding this term:

$$\begin{aligned} \Delta_{\text{orig}} - \Delta_{\text{swap}} &= [S(f_q(Q), f_i(I^+)) - S(f_q(Q), f_i(I^-))] \\ &\quad - [S(f_i(Q), f_q(I^+)) - S(f_i(Q), f_q(I^-))] \end{aligned}$$

For this difference to approach zero over the entire data distribution, the individual similarity functions must converge, i.e.,:

$$S(f_q(Q), f_i(I)) \approx S(f_i(Q), f_q(I)) \quad \forall Q, I \quad (18)$$

This directly implies the minimization of the alignment error  $\mathcal{A}(\theta_q, \theta_i)$  as defined in the lemma.  $\square$

### B.3 Proof of Lemma 3.3

PROOF. Anisotropy can be quantified by the condition number of the embedding covariance matrix  $\Sigma = \text{Cov}(f(X))$ , i.e.,  $\mathcal{H} = \lambda_{\max}(\Sigma)/\lambda_{\min}(\Sigma)$ . A high  $\mathcal{H}$  implies embeddings occupy a low-dimensional subspace.

Without  $\mathcal{L}_{\text{swap}}$ , the model can minimize  $\mathcal{L}_{\text{original}}$  by creating two separate anisotropic cones for queries and items, i.e., finding  $\Sigma_q$  and  $\Sigma_i$  that are individually ill-conditioned.

The inclusion of  $\mathcal{L}_{\text{swap}}$  forces a shared semantic structure. This imposes a consistency constraint on the covariance matrices, as the query encoder must handle the item distribution and vice versa. The optimization is incentivized to find a solution where the covariance structures are compatible:

$$\text{Cov}(f_q(Q \cup I)) \approx \text{Cov}(f_i(Q \cup I)) \quad (19)$$

This constraint makes it difficult to maintain separate, ill-conditioned subspaces. Instead, the model is pushed to utilize the embedding dimensions more uniformly, resulting in a lower condition number  $\mathcal{H}$  and a more isotropic space.

More formally, consider the combined covariance matrix:

$$\Sigma_{\text{combined}} = \frac{1}{2} (\text{Cov}(f_q(Q \cup I)) + \text{Cov}(f_i(Q \cup I))) \quad (20)$$

The swap loss encourages the individual covariance matrices to be close to this combined matrix, preventing extreme anisotropy in either tower's representation space.  $\square$

### B.4 Proof of Theorem 3.4

PROOF. Let the ideal search be  $i^* = \arg \max_I S(f_q(Q), f_i(I))$ . The ANN search approximates this by first selecting a candidate set  $C_Q = \{I \mid \mathcal{P}(f_q(I)) \in \mathcal{K}_Q\}$ , where  $\mathcal{P}$  is the cluster assignment function and  $\mathcal{K}_Q$  is the set of probed clusters for query  $Q$ . Inconsistency arises when  $i^* \notin C_Q$ .

Our proposed training and indexing method minimizes the probability of this event through three key mechanisms:

- (1) From the encoder equivalence induced by representation alignment (Lemma 3.2), we have  $f_i(I) \approx f_q(I)$ . The search objective is therefore well-approximated by an intra-tower problem:

$$\arg \max_I S(f_q(Q), f_i(I)) \approx \arg \max_I S(f_q(Q), f_q(I)) \quad (21)$$

- (2) From the anisotropy reduction (Lemma 3.3), the embedding space of  $f_q$  is more isotropic. In such a space, dot product similarity is strongly correlated with Euclidean distance for normalized vectors:

$$\arg \max_I S(f_q(Q), f_q(I)) \approx \arg \min_I \|f_q(Q) - f_q(I)\|_2 \quad (22)$$

- (3) The ANN coarse search, which selects clusters based on  $\min_{IC} \|f_q(Q) - IC\|_2$ , where  $IC$  are centroids of  $\{f_q(I)\}$ , is a quantized approximation of the RHS of the equation above.

Thus, the coarse search objective becomes a valid proxy for the true ranking objective, ensuring retrieval consistency. The approximation error decreases as the number of clusters increases and the representation alignment improves.  $\square$

## B.5 Proof of Corollary 1

PROOF. The dual-tower enhanced implementation maintains consistency through:

- (1) **Coarse clustering consistency:** The structural vectors  $\{e_j^q\}$  are used for cluster assignment, ensuring alignment with query encoding as established in Theorem 3.4.
- (2) **Residual semantic preservation:** The hybrid-space residual computation  $r_I = e_I^i - c_{k(I)}$  preserves semantic relationships due to  $e_I^i \approx e_I^q$  from representation alignment (Lemma 3.2). This ensures that:

$$\|e_Q^q - e_I^i\| \approx \|e_Q^q - e_I^q\| + \|r_I\| \quad (23)$$

- (3) **Enhanced quantization:** The representation vectors  $\{e_j^i\}$  potentially capture richer item-specific information, leading to more accurate residual quantization while maintaining the unified space constraint through the hybrid-space formulation.

The combination of these factors ensures that retrieval consistency is maintained while quantization accuracy is improved through the dual-tower synergy.  $\square$

## B.6 Detailed Collapse Analysis for Linear Model

The total gradient for the linear model is:

$$\frac{\partial \mathcal{L}_{\text{total}}}{\partial W_q} = W_i [\Delta i q^\top + \lambda q \Delta i^\top] \quad (24)$$

where  $\Delta i = i^- - i^+$ .

We analyze the conditions under which the swap loss contribution becomes redundant:

**B.6.1 Collapse Condition 1:  $\lambda = 0$ .** When  $\lambda = 0$ , the swap loss has no weight, and the total gradient degenerates to:

$$\frac{\partial \mathcal{L}_{\text{total}}}{\partial W_q} = W_i \Delta i q^\top \quad (25)$$

This is identical to the original gradient, and the swap loss produces no optimization effect.

**B.6.2 Collapse Condition 2: Vector Parallelism ( $q \parallel \Delta i$ ).** When the query vector  $q$  is parallel to the document difference vector  $\Delta i$  (i.e.,  $q = \alpha \Delta i$  for some scalar  $\alpha$ ), the symmetrization operator degenerates:

$$M(q, \Delta i) = \frac{1}{2}(q \Delta i^\top + \Delta i q^\top) = \frac{\alpha + 1}{2} \Delta i \Delta i^\top \quad (26)$$

The total gradient becomes:

$$\frac{\partial \mathcal{L}_{\text{total}}}{\partial W_q} = W_i [\Delta i q^\top + \lambda q \Delta i^\top] = W_i (\alpha + \lambda \alpha^2) \Delta i \Delta i^\top \quad (27)$$

This is proportional to the original gradient, making the swap gradient redundant.

**B.6.3 Collapse Condition 3: Special Orthogonal Conditions.** When  $W_i q$  and  $W_i \Delta i$  are orthogonal in the transformed space, the two gradient directions may produce cancellation effects in certain dimensions. Specifically, if:

$$(W_i q)^\top (W_i \Delta i) = 0 \quad (28)$$

then the outer products  $\Delta i q^\top$  and  $q \Delta i^\top$  have orthogonal row spaces in the transformed domain, potentially leading to dimensional cancellation.

**B.6.4 Practical Implications.** In practice, these collapse conditions are rarely fully satisfied:

- $\lambda$  is typically set in  $[0.1, 1.0]$ , avoiding complete removal of swap loss
- Queries and items typically come from different semantic spaces with different statistical properties, making  $q$  and  $\Delta i$  rarely completely parallel
- The orthogonal condition requires specific geometric relationships that are unlikely to hold across the entire dataset

Therefore, the swap loss generally provides meaningful complementary optimization signals that promote representation space alignment in practical scenarios.

Received 20 February 2007; revised 12 March 2009; accepted 5 June 2009